CARBIDE CHARACTERIZATION IN SINGLE AND DOUBLE STEP INOCULATED THIN WALL DUCTILE IRON

[*]Ochulor, E. F[1], Adeosun, S. O[2], Ekeleme, J. U[3], and Ugboaja, J. O[4], Nnaji, R. N[5]

[1-5.] Department of Metallurgical and Materials Engineering, University of Lagos, Akoka, Lagos, Nigeria

*Corresponding Author: eochulor@unilag.edu.ng +234 803 334 5451

ABSTRACT:

Heterogeneous nucleation of graphite is an important aspect of cast iron metallurgy. This is adequately achieved by inoculation treatments, however due to thickness reduction in Thin Wall Ductile Iron (TWDI), carbide precipitation with poor nodularity and nodule count occur in microstructure. Understanding the characteristics of these carbide precipitates regarding type, composition, morphology, and hardness are necessary if use of TWDIs for automotive application is to be sustained. This study produced 3 mm TWDIs castings subjected to pre (single step) and pre/post (double step) inoculation treatments. The ferrosilicon (FeSi) inoculant was varied during melt treatment to capture a wide range of carbide precipitates. Microstructure of samples was investigated using Optical and Scanning Electron Microscopy (SEM). Vickers microhardness tester was employed to evaluate hardness properties. Spot Energy Dispersive Spectroscopy (EDS) was conducted on carbide precipitates to determine composition, also nodularity and nodule counts were estimated. The results indicated that cast samples contained higher volumes of carbides in pre-inoculated melts than those subjected to both pre and post inoculated treatments. Significant portion of carbide precipitates appeared plate-like in shape. Higher Vickers hardness (HV) values correspond to higher volumes of carbide precipitates, 310HV and 382HV for 2.5 and 1.5 wt. % Si respectively for the pre-inoculated samples; while 299 HV and 263 HV for 2.7 and 3.7 wt. % Si respectively for pre and post inoculated samples. The as-cast 3 mm TWDI samples contained M_3C type eutectic carbides (Fe_3C) with plate-like morphology.

Keywords: Carbide precipitates, ferrosilicon, pre-and post-inoculation, microstructure.

INTRODUCTION

Carbides formed during casting are called primary carbides while secondary carbides formed during heat treatment are extremely fine carbides, and strengthen the matrix (Serna *et al.*, 2006). Carbides are important constituent in cast irons (CIs) especially white cast irons (WCIs), where its volume fraction can reach up to 40%, and its type, chemical composition, amount, size, shape and distribution all have significant influence on mechanical properties of the iron. Six kinds of carbides can be formed in steels as shown in Table 1, where M denotes the carbide-forming element. The carbides in Group I have a complicated crystal structure, such as cementite (Fe_3C), or $Cr_{23}C_6$. A specific structural feature of the carbides of Group II as interstitial phases is a simple crystal lattice e.g. TiC, WC, NbC and Mo_2C (Serna *et al.*, 2006).

Table 1: Carbide types in Steel (Serna *et al.*, 2006)

Group I carbides	**Group II carbides**
M_3C	MC
$M_{23}C_6$	M_2C
M_7C_3	
M_6C	

Iron carbide also referred to as cementite is an intermetallic compound of iron (Fe) and carbon (C), an intermediate transition metal carbide with the formula Fe_3C and contains 6.67% C and 93.3% Fe with an orthorhombic crystal structure (Smith and Hashemi, 2006). The hardness difference can be used to identify the carbide types as well as the characterization of its morphology. MC carbides is in the range 2300-2500HV, while that of M_6C is 1400-1600HV. The M_6C grows in the form of fish- bone while the fan-like morphology typifies the mixture of M_6C and MC carbides (Fredriksson and Brising, 1976). Atomic element contrast in the scanning electron microscope (SEM) can also be used for carbide identification, where M_6C shows light grey to white, M_2C is dark grey and MC is black (Karagoz *et al.*, 1989).

Apart from WCIs, ductile irons (DIs) is another type of cast iron, with ternary Fe-C-Si structure, where graphite is in the form of nodules owing to magnesium addition, which is the spheriodizing element. TWDIs are profiles with thickness < 4 mm (Gorny and Tyrala, 2013), dispersed carbides in either lamellar or spherical form plays an important role in providing strength and wear resistance in as-cast pearlitic and heat-treated irons. In ductile iron (DI), carbide content has both direct and indirect effects on the properties of DI castings. Carbide increases the yield strength with the dynamic elastic modulus, reduces the tensile strength, produces a decrease in elongation and significantly reduces machinability. The formation of eutectic carbide during solidification affects the volume fraction of graphite produced as carbide and graphite compete for the carbon contained in liquid iron (Davis, 1996).

Alloying elements in cast irons are categorized into graphitizing elements and carbide promoting elements. The undesirable carbides in TWDIs occur from poor melt processing techniques such as increase in cooling rate owing to section reduction, poor inoculation and nodularization practices, melt chemistry i.e., inadequate carbon equivalence, CE (Sangame and Shinde, 2013). On the other hand, WCIs and high chromium cast irons (HCCIs) have high abrasion resistance

due to the presence of brittle M_7C_3 and/ or M_3C of carbides (Tabrett and Sarre, 2000; Zhi *et al.*, 2008; Yilmaz, 2007). The type, size, morphology and distribution of these carbides control their wear resistance and toughness.

Thus there is need to characterize these carbide precipitates in TWDI for better understanding of their types, sizes, morphology, distribution and consequently the hardness property as developed in cast components. The knowledge of these information is useful in designing the heat treatment procedure for carbide reduction or elimination (Caldera *et al.*, 2013) and for further processing where wear resistance impacted by the carbide phase is desired (Gumienny, 2013; Sellamuthu *et al.*, 2018). Also, during machining of these components, these carbides precipitates influence final surface finish and tool life. Wear resistance applications of carbides in reinforced DI include surface hardened automotive parts such as pistons for compressors, gears, crankshafts; mining; fishing and agricultural industries (Martinez Celis *et al.*, 2011; Dhanapal and Ibrahim, 2016).
From previous studies, there have been focus on solidification kinetics that generate these carbide phases and their impact on mechanical properties. Literature on carbides characteristics in ferrous alloys, steels and high chromium white cast irons (HCWCIs), however, report on carbide types, sizes, morphology, composition and distribution in as cast TWDIs is scanty. Thus, to ensure continued use of TWDI to produce automotive components, there is need to bridge this information gap. Therefore, this study is aimed at investigating the types, morphology, distribution, chemical composition and consequently the hardness of precipitated carbides in pre-and pre/post inoculated 3 mm TWDI cast components.

MATERIALS AND METHODS

The samples were cast at the foundry shop of Machine Tools Osogbo, Osun State Nigeria. The charge materials consisted of cold rolled close annealed (CRCA) steel scrap, ductile iron returns, ferrosilicon alloy and graphite. The chemical compositions of the steel scrap, graphite, ferrosilicon and ferrosilicon magnesium alloys used are shown in the results section.

Green sand molds were made using standard composition requirements of ASTM E2349. A wooden pattern 150 by 150 mm and 3 mm thickness was used to prepare the mold. Melting of the charge materials was done in a 250 Kg capacity dual track, acid lined induction furnace model No.13690/1954.

A 50-kg melt was tapped at 1450^0C into a treatment ladle, the sandwich treatment method was adopted using 1.3 kg ferrosilicon magnesium granules covered with

steel scraps at the bottom of the ladle. After this treatment, the melt was then transferred to the pouring ladle for inoculation treatment. It is important to note that ferrosilicon was used as a charge material and also for inoculation treatment.

Pre-and Pre/post inoculation of Samples

Two 20-kg melt was transferred into two pouring ladles for pre (one step) and pre/post (two step) inoculation. For the pre- inoculation process, varying proportions of the ferrosilicon treatment alloy (inoculant) was placed in the mold cavity prior to coupling. The inoculant proportions and sample designations are shown in Table 2. For the control sample, P0, no inoculation was conducted as only the magnesium treatment was done, afterwards the 3 mm TWDI samples were cast. Pre-and post-inoculation was carried out for the second pouring ladle using in-stream method by introducing the inoculant during transfer of the magnesium treated melt from treatment ladle to pouring ladle. Thereafter, the melt was post inoculated using the in-mold method by placing the various proportions of the inoculant in the mold cavity. This was done before mold coupling and the sample designations are shown in Table 3.

Table 2: Designations for pre-inoculated samples

Sample Designation	P0	P1	P2	P3	P4	P5	P6
Si in Inoculant (Wt. %)	0	1.5	1.7	1.9	2.1	2.3	2.5
Weight of FeSi Inoculant (g)	0	4.4	13.3	17.8	31.2	40.1	49.0

Table 3: Designation for pre-and post-inoculated samples.

Sample Designation	**PP1**	**PP2**	**PP3**	**PP4**	**PP5**	**PP6**
Si in Inoculant (Wt. %)	2.7	2.9	3.1	3.3	3.5	3.7
Weight of FeSi Inoculant (g)	4.4	17.8	40.1	62.4	84.6	106.9

Microstructural Analysis

Samples were sectioned, ground and polished in accordance to ASTM Standard E3-11 for metallographic analysis. The prepared samples were examined in their unetched and etched (using 2% nital solution) conditions a CETI Optical Metallurgical Microscope Model No. 0703552 at magnification of X100 located at the Metallurgical Laboratory, University of Lagos, Akoka, Nigeria. The etched samples were also examined using the JEOL JSM 5900LV Scanning Electron Microscope (SEM), equipped with an oxford INCA^{TM} Energy Dispersive

Spectroscopy (EDS) system. The electron beam was kept stationary at two spots for each sample while spectra were generated, which provides more localized elemental information. Microstructural characterization of nodularity and nodule counts (Equation 1) were carried out using manual procedure as stated in ASTM A247-16 and E407-07 standard procedures. The latter technique (SEM) enabled a detailed observation of the carbide morphology while determination of chemical composition of the carbide precipitates was done using the spot EDS analysis. Chemical composition of the cast samples was analyzed using the optical emission spectroscopy. Nodule Count (graphite nodules/mm^2) is the quantity of nodules per square millimeter on a polished surface examined at X100 magnification.

$$\text{Nodularity } \% = \frac{\text{area (number) of acceptable particles}}{\text{area (number) of all particles}} \; X\ 100 \qquad (1)$$

Hardness Test

Vickers hardness tester was used to evaluate micro hardness properties on the 13 as-cast 3 mm TWDI samples by applying a force of 50Kgf. The test was carried out per ASTM E92-17 standard.

RESULTS AND DISCUSSION

Chemical compositions of charge materials and cast samples

The cast samples in the molding box and after fettling are shown in Figure 1. The chemical compositions of the steel scrap, graphite, ferrosilicon, ferrosilicon magnesium alloys and charge materials used are shown in Tables 4-8 respectively. The chemical compositions of the cast samples are also shown in Table 9. The chemical composition shows manganese and magnesium as the main carbide promoting elements, however their composition is not high enough to cause any harmful effects. Ferro-silicon the main graphitizing element is the main constituent of the ferroalloy inoculant. The variations in the ferro-silicon proportions used in the inoculation affects the residual quantity in the melt, which consequently played a crucial role in the solidification mechanism of the various samples. Increased proportion of inoculant increased the nucleation sites for graphite nodule formation during solidification.

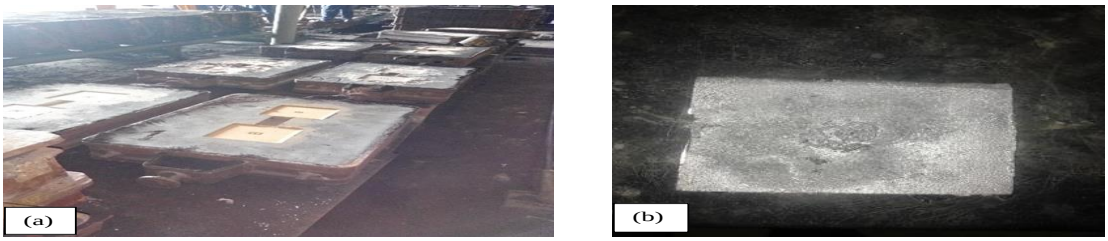

Figure 1: Cast TWDI samples (a) in the molding box (b) after fettling procedure

Table 4: Chemical compositions of the steel scrap (CRCA)

Element	C	S	Mn	P	Fe
wt.%	0.05	0.03	0.3	0.03	96.62

Table 5: Chemical Composition of Graphite

Element	C	Ash	S	Volatile matter	Moisture
wt.%	72	27.5	0.2	<0.5	0.1

Table 6: Chemical composition of Ferrosilicon Alloy (FeSi)

Element	Si	Al	C	S	P	Fe
wt.%	70	0.31	0.0032	0.001	0.001	29.68

Table 7: Chemical Composition of Ferrosilicon Magnesium Alloy (FeSiMg)

Element	Mg	Si	Ca	RE	Al	Fe
wt.%	7.5	44.7	2.02	0.8	<0.7	44.27

Table 8: Chemical Composition of Charge Materials

Charge	Charge (Kg)	Charge (wt. %)	C (wt. %)	Si (wt. %)	Mn (wt. %)
CRCA Scrap	40	80	0.04	0	0.20
Ductile Iron Returns	7.6	15.2	0.54	0.405	0
Ferro Silicon	0.4	0.8	0	0.56	0
Graphite	2.0	4.0	2.88	0	0
Total	50	100	3.55	0.965	0.2

Table 9: Chemical Composition of Cast Samples

Sample Designation	C Wt. %	Si Wt. %	Mn Wt. %	P Wt. %	S Wt. %	Mg Wt. %	Fe Wt. %
P0	3.55	1.22	0.365	0.015	0.007	0.032	94.81
P1	3.49	1.54	0.410	0.016	0.006	0.037	94.50
P2	3.31	1.695	0.365	0.03	0.003	0.029	94.57
P3	3.48	1.93	0.420	0.031	0.014	0.051	94.07
P4	3.47	2.09	0.463	0.041	0.013	0.052	93.87
P5	3.61	2.28	0.460	0.036	0.017	0.044	93.55
P6	3.56	2.51	0.425	0.037	0.016	0.039	93.41
PP1	3.61	2.705	0.313	0.046	0.011	0.036	93.28
PP2	3.59	2.91	0.413	0.042	0.015	0.031	92.99
PP3	3.60	3.11	0.361	0.044	0.012	0.035	92.84
PP4	3.61	3.26	0.39	0.023	0.006	0.032	92.68
PP5	3.59	3.61	0.303	0.009	0.003	0.033	92.45
PP6	3.61	3.68	0.38	0.044	0.011	0.029	92.25

Effect of inoculant proportion on microstructure of pre-and post-inoculated samples

The optical micrographs for the unetched and etched samples are shown in Figures 2-14. Plate-like or needle-like carbide precipitates morphology was observed in all samples except in PP4, PP5 and PP6 arising from metastable transformation due to fast cooling. Final microstructure consisted of graphite nodules formed during eutectic solidification with matrix type made up of ferrite, pearlite or carbides formed from subsequent eutectoid reactions. These transformations depend on rate of carbon diffusion, as fast cooling favors carbide precipitations while slow cooling allows better graphitization during solidification. These plate-like structures were distributed throughout the matrix of the pre- inoculated samples as shown in Figures 3b - 3b micrographs respectively. Carbide precipitates were more pronounced in the P0 (Figure 2b) control sample as no inoculation was implemented. These precipitates progressively reduced with increased proportion of inoculant (Sangame and Shinde, 2013). This suggest that nucleation sites available for the formation of graphite nodules were few. Thus, the formation of more carbide structures was favored in the pre-inoculated samples where only one step inoculation was done. Two step inoculated samples PP1, PP2 and PP3 showed lower volume of carbide precipitation vis–a-vis those observed in the PP set of samples (Mullins, 2006). On the other hand, stable transformation products were observed for PP4, PP5 and PP6 samples (Figures 12, 13 and 14) resulting from increased proportion of silicon i.e. 3.3, 3.5 and 3.7 wt. % respectively in the inoculant used.

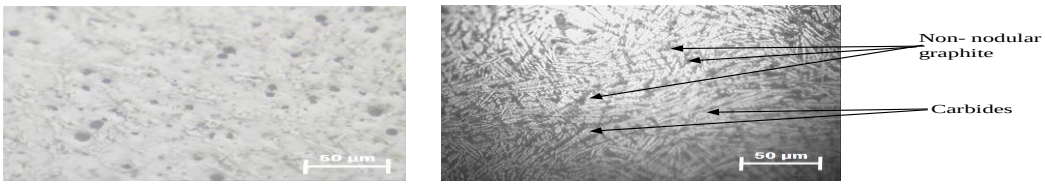

(a) (b)

Figure 2: Optical micrograph of sample P0 (a) unetched (b) etched

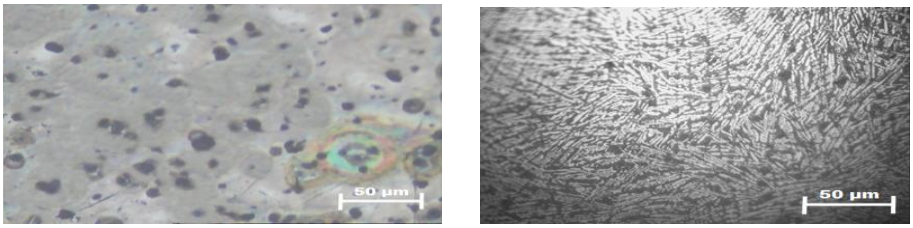

(a) (b)

Figure 3: Optical micrograph of sample P1 (a) unetched (b) etched

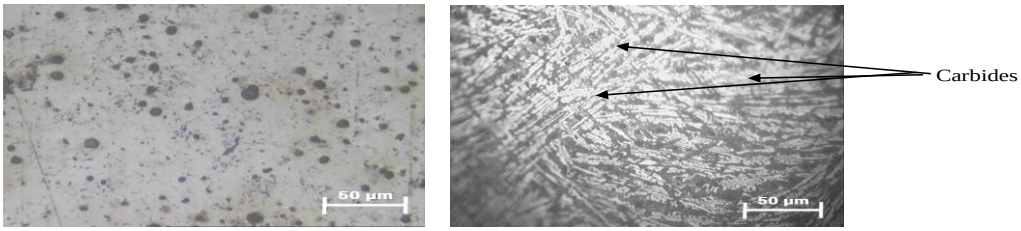

(a) (b)

Figure 4: Optical micrograph of sample P2 (a) unetched (b) etched

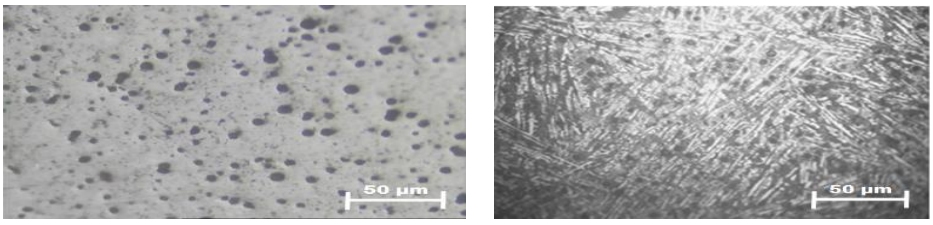

(a) (b)

Figure 5: Optical Micrograph of sample P3 (a) unetched (b) etched

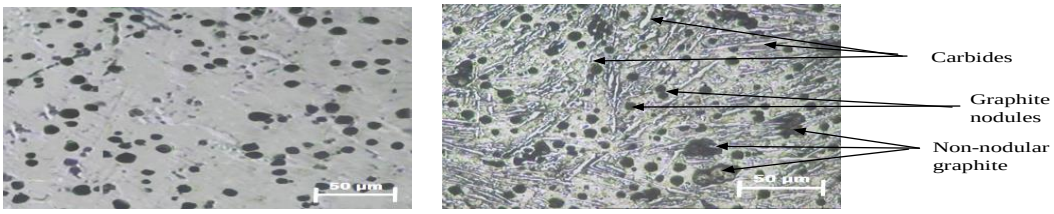

Figure 6: Optical Micrograph of sample P4 (a) unetched (b) etched

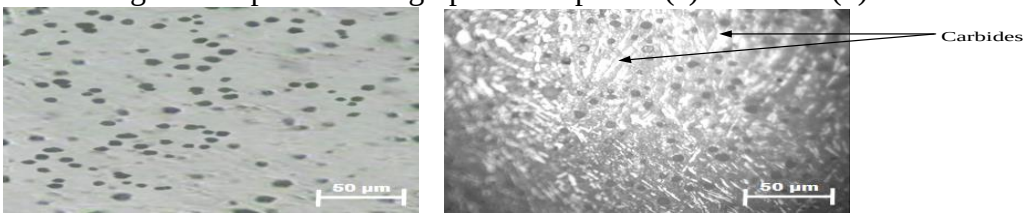

Figure 7: Optical micrograph of sample P5 (a) unetched (b) etched

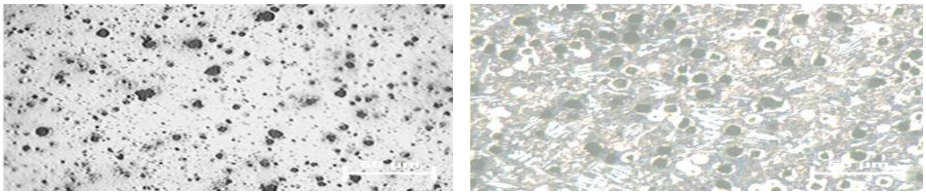

Figure 8: Optical micrograph of sample P6 (a) unetched (b) etched

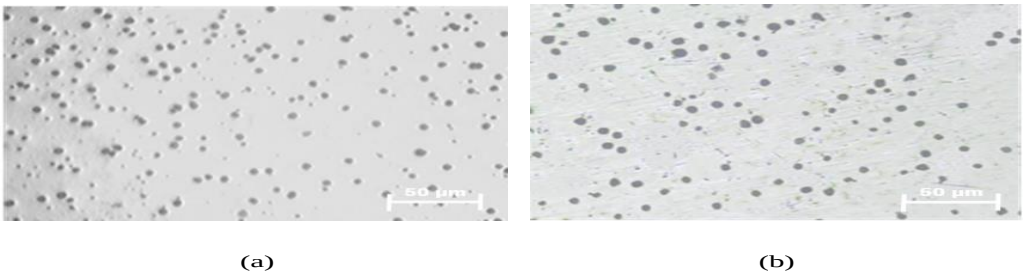

Figure 9: Optical micrograph of sample PP1 (a) unetched (b) etched

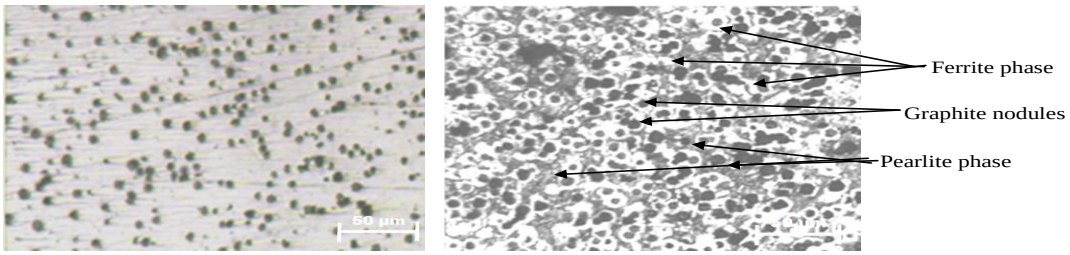

(a) (b)

Figure 10: Optical micrograph of sample PP2 (a) unetched (b) etched

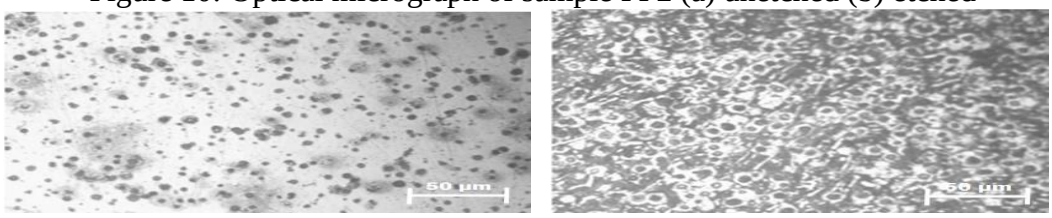

(a) (b)

Figure 11: Optical micrograph of sample PP3 (a) unetched (b) etched

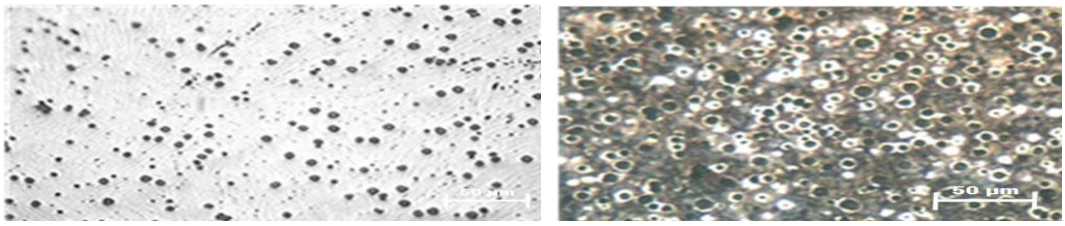

(a) (b)

Figure 12: Optical micrograph of sample PP4 (a) unetched (b) etched

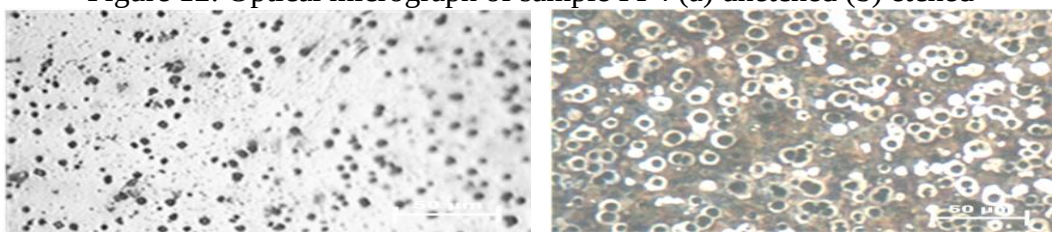

(a) (b)

Figure 13: Optical micrograph of sample PP5 (a) unetched (b) etched

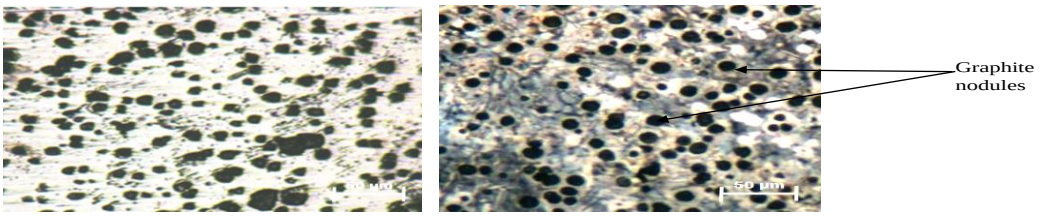

Figure 14: Optical micrograph of sample PP6 (a) unetched (b) etched

Scanning Electron microscopy (SEM)

The SEM micrographs with corresponding EDS are shown in Figures 15-20 for P2, P4, P6, PP1, PP2 and PP3 samples. All the micrographs showed large volumes of carbide precipitations, which appeared as light grey in colour with needle/plate like morphology. Elemental composition from EDS analyses showed high weight percentage of iron (Fe) followed by carbon (C). Estimation of the chemical formula of the carbide precipitate was carried out. This suggested the presence of primary cementite (Fe_3C), of the M_3C -type. In samples P4 and PP3, 93.2 wt. % Fe and 4.3 wt. % C, 89.6 wt. % Fe and 8 wt. % C respectively as the major constituent element. This indicates primary carbide (Fe_3C) in the spectrum.

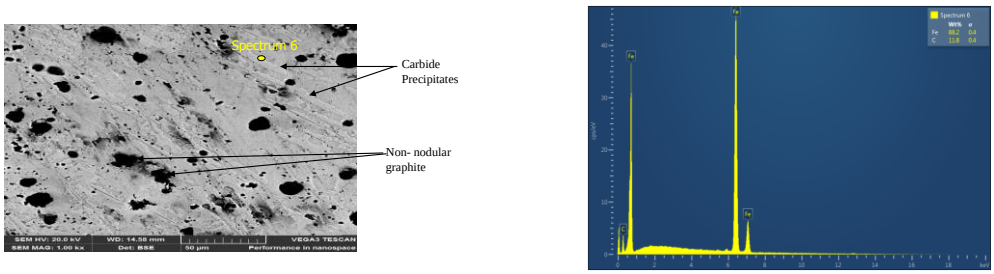

(a) (b)

Figure 15: Sample P2 (a) SEM Micrograph (b) EDS analysis

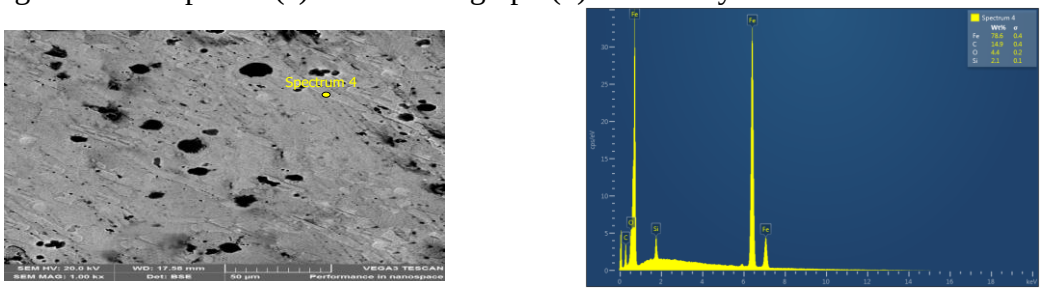

(a) (b)

Figure 16: Sample P4 (a) SEM Micrograph (b) EDS analysis

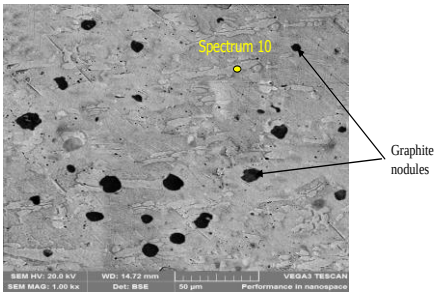

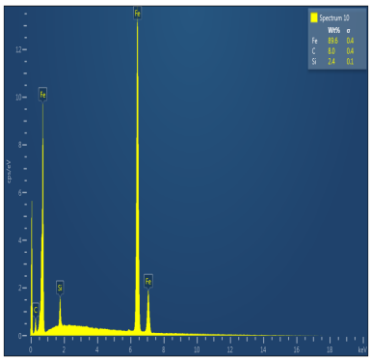

(a) (b)

Figure 17: Sample P6 (a) SEM Micrograph (b) EDS analysis

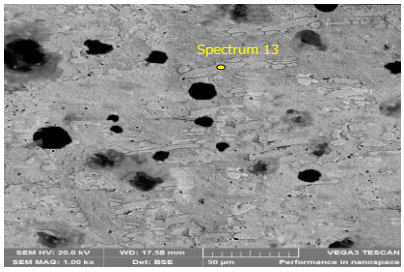

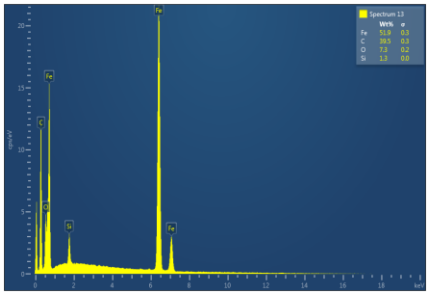

(a) (b)

Figure 18: Sample PP1 (a) SEM Micrograph (b) EDS analysis

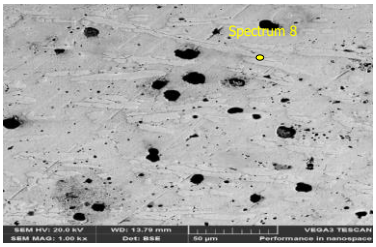

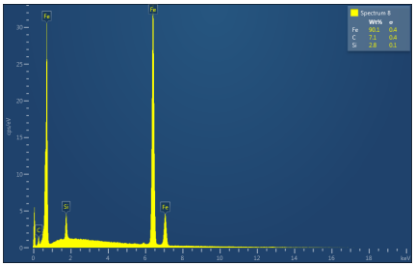

(a) (b)

Figure 19: Sample PP2 (a) SEM Micrograph (b) EDS analysis

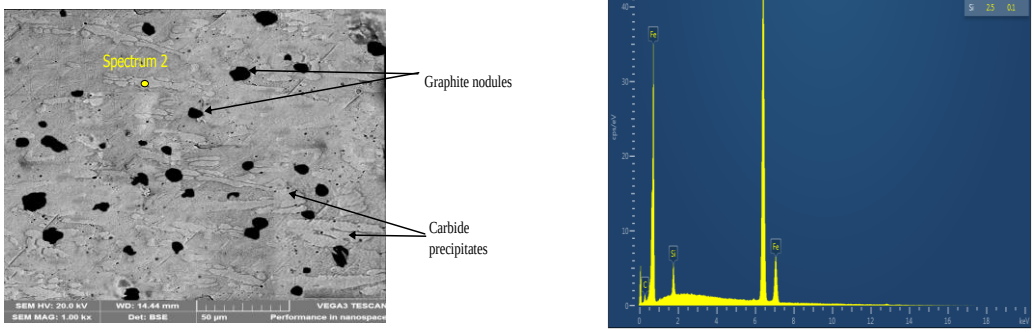

(a) (b)

Figure 20: Sample PP3 (a) SEM Micrograph (b) EDS analysis

Effect of inoculant proportion on Nodularity and nodule count of pre-and post-inoculated samples

The nodularity and nodule count with corresponding ferrosilicon proportion are shown in Table 10 for all cast 3 mm TWDI samples. The nodularity of pre-inoculated samples increased with increasing inoculant proportion. This same trend is observed in the pre- and post- inoculated samples. However, this pattern was not sustained for the nodule count, where it dropped from P0 to P1, P3 to P4, P6 to PP1 and then fell progressively from PP3 to PP6. The pre-and post-inoculated samples generally, showed better nodularity and nodule count values as increased inoculant proportion favored increased graphitization with better nodule characteristics. The consequence is reduction in carbide precipitations. This agrees with the findings of Pedersen and Tiedje, (2008) where sufficient number of graphite nodules are required to avoid formation of carbides during solidification in thin walled castings owing to the high solidification rate.

Table 10: Nodularity and Nodule counts with corresponding ferrosilicon proportion during inoculation for TWDI samples.

Sample Designation	Wt. % Si	Nodularity (%)	Nodule Count (Nod/mm^2)
P0	0	57.3	31
P1	1.5	40.4	29
P2	1.7	52.9	65
P3	1.9	78.8	101
P4	2.1	80.4	95
P5	2.3	82.5	94
P6	2.5	87.4	137
PP1	2.7	92.3	125
PP2	2.9	94.2	301
PP3	3.1	95.1	382
PP4	3.3	96.3	371
PP5	3.5	95.8	367
PP6	3.7	96.7	345

Effect of inoculant proportion on hardness properties of pre-and post-inoculated samples

Plots for Vickers hardness trend for pre-inoculated and pre-and post-inoculated TWDI samples are shown in Figures 21 and 22 respectively. The Vickers hardness gave the highest value of 398HV for the sample P0 where no inoculation was done. Although this was not captured in the plot, however, for the pre-inoculated samples this property followed a decreasing trend with increased proportion of inoculant. P1 has hardness of 382HV, P2 has a lower hardness value

of 354HV and this continues till the last pre-inoculated sample P6, which has lowest hardness of 310HV. This trend is because of the volumes of carbide precipitated as seen in the micrographs (Figures 2-8), which reduces as inoculant proportion increased. The hardness properties for the pre-and post- inoculated samples in Figure 22 also followed this same trend, which decreases from PP1 (299HV) to sample PP2 (292HV) and progressively decreases to PP6 (263HV). Generally, the pre-inoculated samples had higher hardness than the samples that were pre- and post inoculated. This also confirms the significance of inoculation on graphite nodule formation and reduction of carbides in the as cast 3 mm TWDI casting (Bockus *et al.*, 2008).

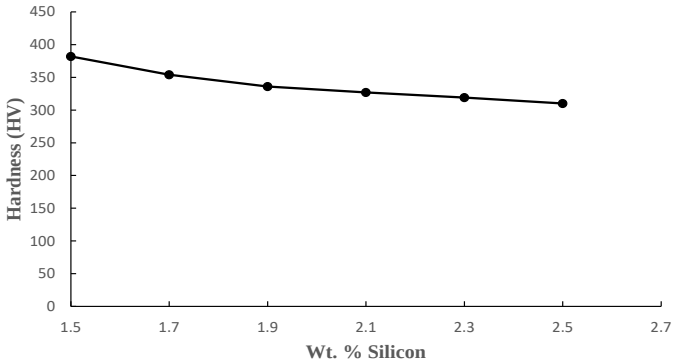

Figure 21: Vickers hardness versus wt. % silicon in inoculant (Pre-inoculation)

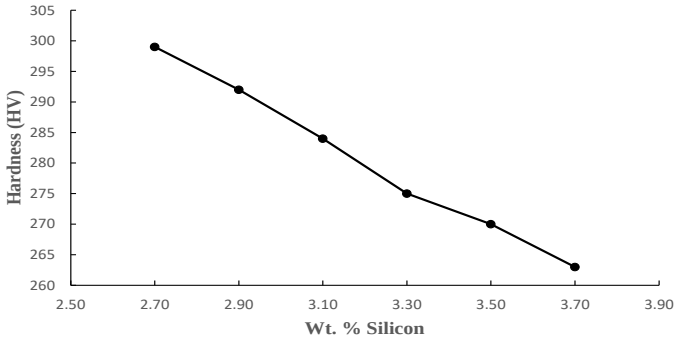

Figure 22: Vickers hardness versus wt. % silicon in inoculant (Pre and post-inoculation)

CONCLUSION

As-cast 3 mm thick thin wall ductile iron (TWDI) are prone carbide precipitations due to thickness reduction Silicon is the main graphitization element in the melt; however insufficient silicon content (in ferrosilicon inoculant) available for inoculation treatment contributed greatly to the formation of carbides as seen in the microstructures of P1 to P6, and PP1 to PP3 samples. These large volume of carbides formed resulted in the high hardness values observed in both pre-inoculated samples (P1 to P6) and in the pre- and post- inoculated samples (PP1 to PP3). On the other hand, the precipitation of carbides was significantly reduced in samples PP4, PP5 and PP6. The shape characteristics of the graphite nodules formed increased with inoculant proportion with P1 having the lowest nodularity (40.4%). Nodularity increase in P6 (87.4%) and PP6 (96.7%). This shows that inoculation plays an important role in nodule formation as it creates nuclei for heterogeneous nucleation of graphite nodules. However, nodule counts did not follow this trend. The SEM of the samples showed needle-like or plate-like carbides morphology, with iron and carbon elements that suggest the formation of cementite (Fe_3C) as earlier observed from the EDS analyses and iron carbon phase diagram.

ACKNOWLEDGEMENT

The authors are gratefully to the Management and Staff of Machine Tools Osogbo, Osun State Nigeria for their assistance in the use of their facilities. The contribution of the Staff of Metallurgical Laboratory of the Department of Metallurgical and Materials Engineering, University of Lagos are also recognized.

REFERENCES

Bockus, S., Venckunas, A and Zalgarys, G. (2008), Relation between Section Thickness, Microstructure and Mechanical Properties of Ductile Iron Castings. *Materials Science,* 14 (2): 115.

Caldera, M., Rivera, G. L., Boeri, R. E. and. Sikora J. A (2013), Precipitation and dissolution of carbides in low alloy ductile iron plates of varied thickness, *Materials Science and Technology,* 21(10): pp 1187-1191.

Davis, J. R. (1996), ASM Specialty Handbook Cast Irons. *ASM International*. The Material Information Society, pp 65-68.

Dhanapal, P. and Ibrahim, A. S. (2016), Production of Carbidic Austempered Ductile Iron (CADI). *International Conference on System, Science, Control, Communication, Engineering and Technology*, pp 527-535.

Fredriksson, H. and Brising, S. (1976), Formation of carbides during solidification of High Speed Steels. *Scandinavian Journal of Metallurgy* 5(6): p 268.

Gorny, M. and Tyrala, E. (2013), Effect of cooling rate on microstructure and mechanical properties of Thin Wall Ductile Iron Castings. *Journal of Materials Engineering and Performance.* 22(1): pp 300-305.

Gumienny, G. (2013), Effects of Carbides and Matrix on the Wear Resistance of Nodular Cast Iron. *Archives of Foundry Engineering*, 13(3): pp 25-29.

Karagoz, S., Liem, I., Bischoff, E. and Fischmeister, H. F. (1989), Determination of carbide and matrix compositions in high-speed steels by Analytical Electron Microscopy. *Metallurgical Transactions A*, 20(12): pp 2695-2701.

Martinez Celis, M., Valle, N., Lacaze, J., Thorbjornsson, I.O., Johannesson, B. and Thorgrimsson, J. T. (2011), Microstructure of As Cast Reinforced Ductile Iron. *International Journal of Cast Metal Research* 24(2): pp 76-82.

Mullins, J. D (2006), The most important part of Ductile Iron Production-Inoculation. *Sorelmetal Technical Services* (88): pp 1-2.

Pedersen, K.M and Tiedje, N.S (2008), Graphite nodule count and size distribution in Thin Walled Ductile Cast Iron. *Material Characterization*, 59(8): pp 1111-1121.

Sangame, B. B. and Shinde, V. (2013), The effect of inoculation on microstructure and mechanical properties of Ductile Iron. IOSR *Journal of Mechanical and Civil Engineering,* 5 (6): pp 17-23.

Sellamuthu, P., Haris Samuel D. G., Dinakaran, D., Premkumar, V. P., Li, Z. and Seetharaman, S. (2018), Austempered Ductile Iron (ADI) Influence of austempering temperature on microstructure, mechanical and wear properties and energy consumption. *Metals 8* (53): pp 1-12.

Serna, M. M., Jesus, E. R. B, Galego, E., Martinez, L. G., Correa, H. P. S. and Rossi, J. L. (2006), An overview of the microstructures present in High Speed Steel Carbides Crystallography. *Materials Science Forum*, (530-531): pp 48-52.

Smith, W. F. and Hashemi, J. (2006), Foundations of Materials Science and Engineering. 4th Edition, McGraw-Hill Higher Education, New York.

Tabrett, C. P. and Sare, I. R. (2000), Fracture toughness of High-Chromium White Iron, influence of cast structure. *Journal of Material Science*, 35: pp 2069-2077.

Yilmaz, S. O. (2007), Wear behaviour of TiB_2 inoculated 20Cr-3Mo-4C High Chromium White Cast Irons. *Journal Material Science* 42 (16): pp 6769-6778.

Zhi X, Xing Y, Gao Y, Fu H, Peng J and Xiao B (2008), Effect of heat treatment on microstructure and mechanical properties of a Ti-Bearing Hypereutectic High Chromium White Cast Iron. *Material Science Engineering A*, 487: pp 171-179.